

Advances in X-ray Analysis, Volume 49

MEASUREMENT OF STRAIN AND LATTICE TILT AT THE MARGINS OF THIN FILM ISLANDS ON SINGLE-CRYSTAL SUBSTRATES BY DOUBLE-CRYSTAL X-RAY TOPOGRAPHY

Paul M. Adams
The Aerospace Corporation, Los Angeles, California 90009

ABSTRACT

Various amounts of strain and lattice deformation were introduced into <111> Si substrates by the deposition of amorphous Si films of different thicknesses. Strain and deformation are concentrated along the film edges and were recorded as contrast in double-crystal X-ray topograph (DXRT) images. The contrast in the DXRT images was measured and was related to lattice deformation by means of the X-ray rocking curve. The technique was able to independently measure deformation from strains and lattice tilts at film edges. These deformations varied linearly with film thickness.

INTRODUCTION

Stress produced during the deposition of the thin films is a major factor which contributes to the failure of optical coatings and electronic devices. The ability to measure film stress is therefore essential for understanding the failure mechanisms of optical films and electronic devices. Double-crystal X-ray topography (DXRT) is a highly sensitive technique for detecting and imaging strains and defects in single crystals. The DXRT method is capable of detecting stresses in films as a result of the strains and deformations that they transmit to the single-crystal substrate. Strain and deformation in the substrate are concentrated along the edges of film islands. These deformations result in local variations in the diffracted X-ray intensity and appear as contrast in the DXRT image. The magnitude of stress in the substrate can be estimated from elasticity theory by taking into account the intrinsic stress in the film [1, 2]. The intrinsic stress in the film island transmits a force per unit length to the substrate at the film edge and produces deformation in the substrate. Intrinsic stresses in films typically develop in films that are deposited at some temperature above room temperature because a difference in the coefficient of thermal expansion exists between the film and substrate.

X-ray topographic techniques have been used in the past to study strain effects associated with the edges of film islands [3-7]. More recently, X-ray microdiffraction has been used to map the deformations produced by film islands [8-11]. Compared with the Lang method [3,5] the DXRT method is a low divergence reflection technique, and for this reason has a much higher sensitivity to strains and deformation, and as a result, different contrast forming mechanisms and expected to predominate.

Extinction, orientation, kinematical, and Borrmann, have all been proposed as contrast forming mechanisms in X-ray topographs [3, 4, 6]. Orientation contrast in DRXT has been described by Bonse [12] and is related to changes, in crystal orientation (lattice tilt /rotation) and interplanar spacing, surrounding defects. Bonse [12] and Bonse and Hartmann [13] have related the contrast in DXRT images to the X-ray rocking curve and have applied the technique to the mapping of strain

This document was presented at the Denver X-ray Conference (DXC) on Applications of X-ray Analysis.

Sponsored by the International Centre for Diffraction Data (ICDD).

DXC Website
– www.dxcicdd.com

ICDD Website
- www.icdd.com

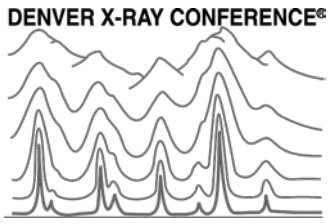

fields, around individual dislocations in silicon and lattice parameter variations and lattice tilts in float-zone grown Si single-crystals. The relationship between contrast in DXRT images is considered to be an approximately linear function of the "combined" local strain (ΔS) and local intensity change (ΔI) by [13]:

$$\Delta I = M\Delta S \quad (1)$$

This applies only to moderate amounts of strain which are represented by ΔI in the linear portion of the rocking curve and where |M| is proportional to the slope of that linear region. The combined strain, by definition (≡), can be represented by [13]:

$$\Delta S \equiv (\Delta d/d) \text{ Tan } \theta_B + n_{gd} \cdot e_t \Delta\theta \quad (2)$$

where Δθ is local lattice rotation, Δd/d is the local lattice parameter change, θ_B is the Bragg angle, and n_{gd} and e_t are unit vectors parallel to the diffractometer axis and axis of lattice tilt respectively. Since the sign of M changes (M > 0, M < 0) depending on the side or wing (+, -) of the rocking curve, the sense of contrast is expected to be reversed if topographs are taken on opposite positions of the rocking curve. Since the sign of $n_{gd} \cdot e_t$ is inverted when the sample is rotated 180° about the Bragg normal, then the contrast in each position (ΔI_+ and ΔI_-) can be related to the contrast associated with lattice rotation ΔI_θ and lattice parameter change ΔI_d by [12]:

$$\Delta I_d \equiv \tfrac{1}{2} (\Delta I_+ + \Delta I_-) \quad (3) \qquad \text{and} \qquad \Delta I_\theta \equiv \tfrac{1}{2} (\Delta I_+ - \Delta I_-) \quad (4)$$

Symmetric parallel sided film islands are a special case, since the opposite sense of lattice tilt exists on opposite film edges and produces the same effect as if a single film edge was rotated 180° and reimaged. In this way, by taking topographs with the sample at several positions on the rocking curve it would be possible to determine lattice parameter changes due to strain (Δd/d) and tilts (Δθ) separately.

EXPERIMENTAL

Sample substrates were <111> single-crystal silicon (2.54 cm dia and 3.2 mm thick). Contrast effects in DXRT images are at a maximum at film island edges are perpendicular with the incident x-ray beam. Back-reflection Laue photographs were used to orient each substrate, identically with the film mask before film deposition, with the long dimension of the island perpendicular to the beam for the (511) reflection. Two amorphous silicon film islands (3 mm x 6 mm) were deposited on each of four substrates by planar magnetron sputtering. Film thicknesses measured with a Dektak IIA contact profilometer were 211 nm, 435 nm, 599 nm and 779 nm.

The (511) reflection was selected for the DXRT studies because it offers a favorable geometry for recording the topographic image with a minimum of distortion. A computer controlled Blake double-crystal diffractometer configured in the (+, -) unequispacing mode using copper radiation and a (100) Ge monochromator was used to acquire all DXRT images. The monochromator was aligned for the (422) reflection for all topographic work, and the $K_{\alpha 1}$ component was selected by means of two slit systems. DXRT images were taken of all four film samples at 1/3, 1/2 and 2/3 maximum intensity positions on both (+) and (-) Δθ positions on the rocking curve, as well as at

the maximum peak intensity. The exposure times of these topographs were varied (15-60 min) in an attempt to produce a similar grey level in the background of each topograph. Ilford L-4 nuclear emulsion film with a 50-micron thick emulsion layer was used for recording all DXRTs. Scanning densitometer traces were performed with a Jarrel-Ash densitometer interfaced with a microcomputer. The topograph plates were scanned (1mm/min) with a 25 μm x 250 μm slit aperture positioned parallel with the long dimension of the island.

RESULTS

Figure 1 represents a series of (511) topographs of the 435 nm thick film island taken at various positions on the rocking curve and it can be seen that the type of contrast varies markedly depending on the position of the rocking curve at which it was exposed. It can be seen that the sense of contrast in the DXRT image is reversed on opposite film edges and reflects the different sense of lattice tilt at each edge with respect to the incident x-ray beam. The interpretation of these topographs however,

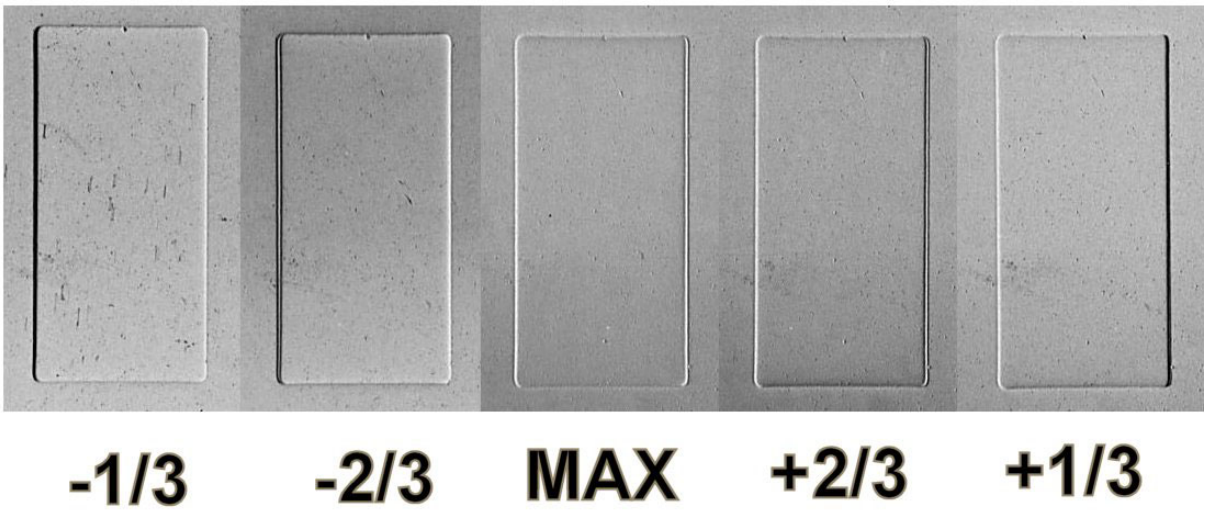

Figure 1. DXRT images of 435 nm thick film island taken at Δθ positions corresponding to 1/3X, 2/3X, 1X the maximum intensity on the rocking curve (-/+ denote -/+Δθ sides of the rocking curve, respectively).

is consistent with the model that the contrast (ΔI) at opposite film edges is related to a Δθ lattice change which consists of two parts; one from strain ($\Delta\theta_d$) and one from lattice tilt ($\Delta\theta_\theta$). Since the strain at each film edge is the same, but the sense of lattice tilt is opposite, but of the same magnitude, then by rearranging equations (3) and (4), the Δθ observed at film edges (1) and (2) is given by:

$$\Delta\theta_1 = \Delta\theta_d + \Delta\theta_\theta \quad (5) \qquad \text{and} \qquad \Delta\theta_2 = \Delta\theta_d - \Delta\theta_\theta \quad (6)$$

and the contrast in the topographs can easily be interpreted by means of the rocking curve if it is assumed that $\Delta\theta_\theta$ is larger than $\Delta\theta_d$. For example; assuming a rocking curve such as that in Figure 2 where topograph images have been recorded at positions A, B, and C and $\Delta\theta_1$(-) and $\Delta\theta_2$(+) are the maximum lattice change given by the above; then one would expect the following contrast to appear

at film edges (1) and (2): At position A, film edge (2) would display negative contrast (lower intensity) since the local lattice is at a position lower down on the rocking curve, whereas edge (1) would exhibit positive contrast with some maximum corresponding to $\Delta\theta_1$. At position B both edges would display negative contrast, with edge (2) displaying more than edge (1). At position C, film edge (1) displays negative contrast. Film edge (2), however, shows some interesting results. The $+\Delta\theta$ associated with this edge takes it through the maxima (positive contrast) and down the opposite side of the rocking curve and past the corresponding intensity at position C (relative negative contrast). Since the maximum lattice change must return to zero at some distance from

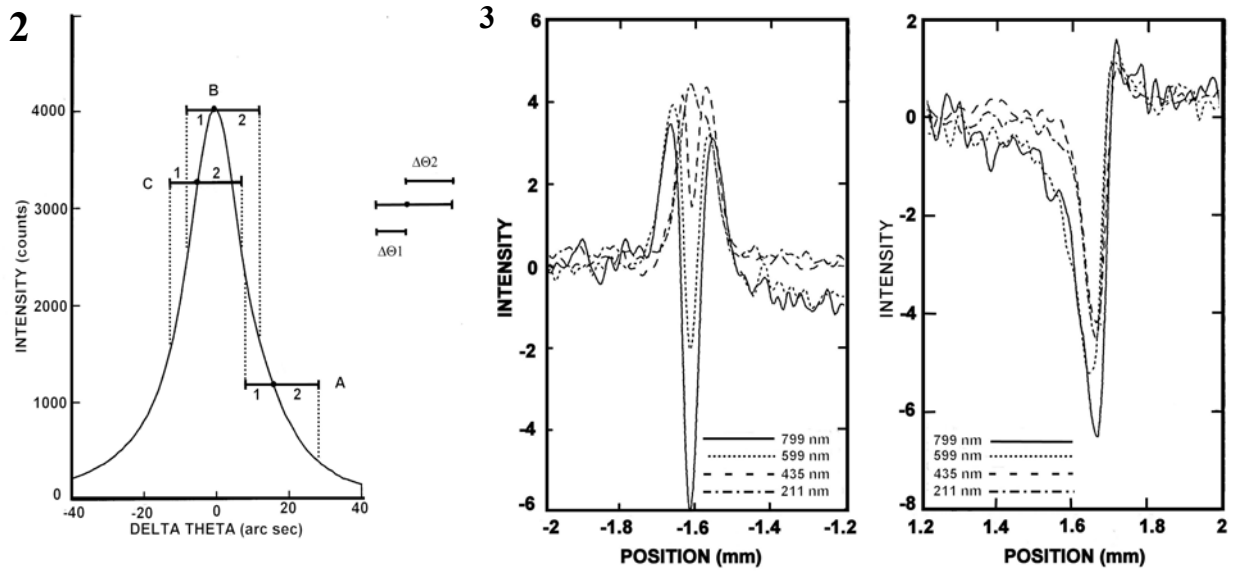

Figure 2. Schematic rocking curve explaining interpretation of DXRTs of film islands.
Figure 3. Densitometer traces across film edges at –2/3 position on the rocking curve.

the film edge, then one would expect the contrast pattern to be repeated. The result is two positive contrast (dark) bands, which represent the local lattice orientation equivalent to the rocking curve maximum, separated by a region of relative negative contrast. The degree of relative negative contrast will depend upon whether or not the $\Delta\theta$ position exceeds the point on the opposite side of the rocking curve equivalent to the one at which the topograph was exposed. This interpretation accounts for the contrast features observed in the (511) topographs, and explains why double positive contrast features are observed at film edges at some positions of the rocking curve. These double positive contrast features indicates that the lattice deformations observed are much larger than the linear portion of the rocking curve and, for this reason, the method of interpreting contrast in DXRT images used by Bonse and Hartmann [13] cannot be used.

Figure 3 displays scanning densitometer traces of topographs of all four samples taken at the same position on the rocking curve. It can be seen that the contrast at the film edges changes as a function of film thickness and that the observed curves are consistent with $\Delta\theta$ increasing with increasing film thickness. By using the approach outlined above it was possible to obtain an estimate of the maximum combined $\Delta\theta$ lattice distortion associated with the film edges. All topographs, taken at each position on the rocking curve, were examined and interpreted. The data at film edges exhibiting only negative contrast were ignored because of the limited range of $\Delta\theta$ possible with the measurement. The averages of this data were assembled and are given in Figure 4 as a plot of $\Delta\theta$

vs. film thickness. It can be seen that there is a difference between the sign (or sense) and magnitude of Δθ observed on opposite film edges, and that each is a linear function of film thickness. The film edge (1), closest to the incident X-ray source, exhibits a +Δθ lattice change while edge (2) displays a - Δθ change. This is consistent with the sense of lattice tilt expected from films being in compression, as was measured by an interferometric technique using similar films deposited on thin deformable substrates. There is some deviation from linearity and greater uncertainty associated with the thickest film because the observed Δθ covers a major portion of the rocking curve and it is

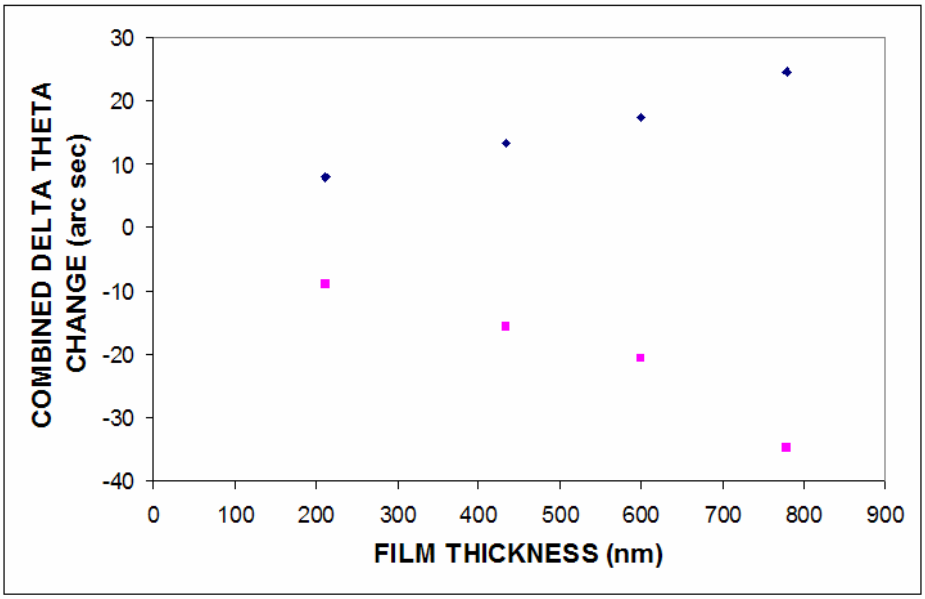

Figure 4. Combined Δθ changes at film island edges. $\Delta\theta_1$ = diamonds, $\Delta\theta_2$ = squares.

difficult to estimate Δθ as a function of intensity on the low intensity wings of the rocking curve. From the differences in Δθ observed at opposite film edges it is possible to determine the separate contributions of strain ($\Delta\theta_d$) and lattice tilt ($\Delta\theta_\theta$) from equations 5 and 6. The results are given in Figure 5. The analysis shows that lattice tilt is the predominant deformation associated with these film edges. Both strain and lattice tilt appear to be linear functions of thickness over the range of film thicknesses studied.

CONCLUSIONS

A technique was developed to interpret the image contrast in (511) topographs, based on the rocking curve, and to measure the individual components of lattice tilt and strain at the margins of film islands. Film islands represent a simplified and ideal case of stresses, strains, and lattice tilts being introduced into a single crystal substrate by a film. The interpretation was not as straight forward as that used by Bonse and Hartmann [13] because of the large lattice deformations that were observed. Nevertheless, this technique was able to independently measure deformation from strains and lattice tilts at film edges. In this case where the film islands are large, with respect to the deformations, and the substrates are thick, the deformations varied linearly with film thickness. The DXRT method is also able to determine whether compressive or tensile stresses were present in a film and may be a useful tool for measuring the intrinsic stress in film islands deposited on rigid substrates.

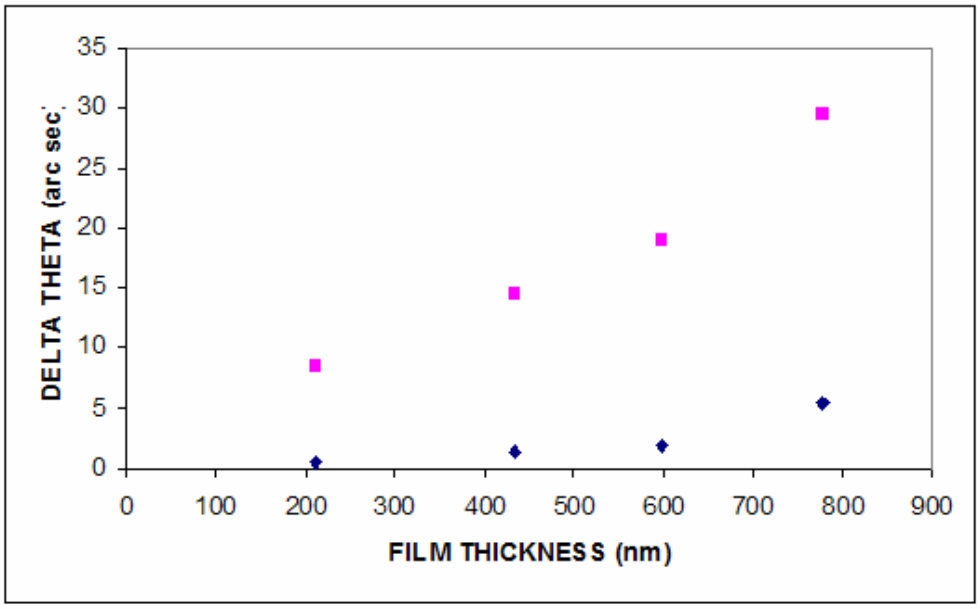

Figure 5. Calculated Δθs from lattice tilts (squares) and lattice strain (diamonds).

ACKNOWLEDGEMENTS

This study was supported by The Aerospace Corporation IR&D Program. The author would like to thank W. Burns and B. Sinshiemer for the growth of the Si films.

REFERENCES

1. Hu, S. M., *J. Appl. Phys.,* **1979**, 50, 4661-4666.
2. Jain, S. C.; Maes, H. E.; Pinardi, K.; De Wolf, I., *J. Appl. Phys.,* **1996**, 79, 8145-8165.
3. Meieran, E.; Blech, I., *J. Appl. Phys*., **1965**, 36, 3162-3167.
4. Meieran, E.; Blech, I, *Phys. Stat. Sol.*, **1968**, 29, 653-667.
5. Blech, I.; Meieran, E, *J. Appl. Phys.*, **1967**, 38, 2913-2919.
6. Schwuttke, G.; Howard, J., *J. Appl. Phys.*, **1968**, 39, 1581-1591.
7. Saccocio, E., *J. Appl. Phys.*, **1971**, 42, 3619-3624.
8. Nishino, Y.; Imura, I., *Phys. Stat. Sol (A),* **1982**, 74, 193-200.
9. Murray, C.; Noyan, I. C.; Lai, B.; Cai, Z., *Powder Diffraction*, **2004**, 19, 56-59.
10. Murray, C.; Noyan, I.; Mooney, P.; Lai, B.; Cai, Z., Appl. Phys. Lett., **2003**, 83, 4163-4165.
11. Noyan, I; Wang, P-C.; Kaldor, S.; Jordqan-Swet, J., Appl. Phys. Lett., **1999**, 74, 2352-2354.
12. Bonse, U, *Direct Observation of Imperfections in Crystals* (ed. by J. Newkirk and J. Wernick), John Wiley, New York, 1962, 431-460.
13. Bonse, U.; Hartmann, I., *Zeits. fur Kristall.*, 1981, 156, 265-279.